Assessing Mars Curiosity Rover Wheel Damage

Arturo Rankin, Nikunj Patel, Evan Graser, Jiun-Kai Freddy Wang, Kimberly Rink
Jet Propulsion Laboratory, California Institute of Technology
4800 Oak Grove Dr.
Pasadena, CA 91109
(818) 354-9269
arankin@jpl.nasa.gov

***Abstract*—An alarming rate of wheel skin cracks was first observed on the Mars Science Laboratory (MSL) Curiosity rover about 14 months after the start of its surface mission. Nine years later (as of August 2, 2021), Curiosity has four broken wheel grousers, three on the left middle wheel and one on the right middle wheel. There are a substantial number of wheel skin cracks on the left front, left middle, and right middle wheels such that the number of grousers on each that are considered at risk of breaking are 10, 7, and 11, respectively. Although the current level of wheel damage does not significantly limit Curiosity's mission objectives, a higher damage rate could impact surface operations, so the damage rate is closely monitored. On November 30, 2013, the MSL Surface Operations team began periodically acquiring images of Curiosity's wheels. In this paper, we describe the process the Mobility Operations team uses to assess wheel damage, the current state of Curiosity's wheels, and how the wheel damage assessments have influenced driving guidelines and wheel imaging frequency.**

TABLE OF CONTENTS

1. INTRODUCTION

The Mars Science Laboratory (MSL) Curiosity rover landed on Mars on August 6, 2012 and driving commenced seventeen Martian solar days (sols) later. As of sol 3195, Curiosity has driven 26,256 m over a variety of terrain types and slopes [1]. The previous Mars rovers, Mars Pathfinder (MPF) Sojourner [2] and Mars Exploration Rovers (MER) Spirit and Opportunity [3], did not experience any wheel damage during their lifetimes. In October 2013, the Curiosity Operations team observed significant wheel damage after less than 4 km of driving. Lessons learned from the resulting investigation into the causes of the damage informed the redesign of the wheels for the Mars 2020 (M2020) Perseverance rover, which landed on Mars on February 18, 2021, and no wheel damage has been observed in its first eight months of driving.

Figure 1 illustrates the size differences between a MPF, MER, and MSL rover and their wheels, and Table 1 compares key wheel specifications for MPF, MER, MSL, and M2020. The

978-1-6654-3760-8/22/$31.00 ©2022 IEEE

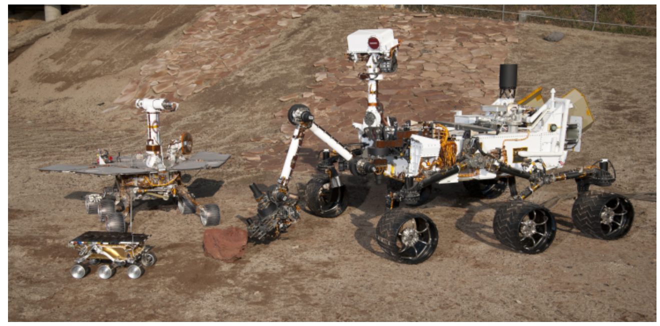

Figure 1. MPF (left), MER (middle), and MSL (right) flight-like testbed rovers in the Jet Propulsion Laboratory (JPL) Mars Yard, illustrating the size differences between the rovers and their wheels. Image Credit: NASA/JPL-Caltech.

Table 1. Comparison of Mars rover mass and wheel specifications.

	MPF	MER	MSL	M2020
Rover mass	11.5 kg	185 kg	899 kg	1,025 kg
Wheel diameter including grouser	14 cm	26.2 cm	50.0 cm	52.3 cm
Wheel width	7.9 cm	21.5 cm	40.0 cm	33.6 cm
Wheel surface thickness	0.2 mm stainless steel	3.25 mm aluminum	0.75 mm aluminum	1.651 mm aluminum
Wheel grousers	34 rows of spot-welded stainless steel cleats	25 straight grousers	19 chevroned grousers plus 8 straight grousers	48 gently curved grousers

size of the MSL and M2020 rovers are nearly identical with the M2020 rover being 126 kg heavier. The surface of each of Curiosity's six identical wheels consists of 19 cleat-like features (called grousers) across the entire width of the wheel for traction, a set of odometry features that leave a distinctive pattern for performing visual odometry (VO) on otherwise featureless terrain, and a thin layer of skin (0.75 mm). Each grouser contains four chevron features designed to mitigate wheel side slippage. Other features that provide structural strength are a vertical rim on each edge of the wheel and a stiffening ring around the interior of the wheel, located two-thirds of the wheel width from the inside edge of the wheel. A drive actuator is attached to each wheel's stiffening ring by

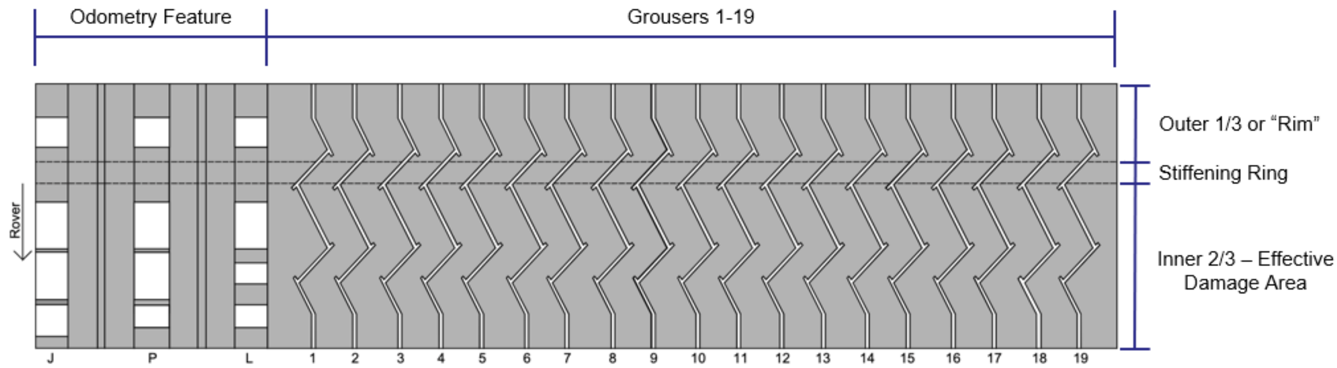

Figure 2. An unrolled MSL wheel. Each wheel contains 19 grousers and an odometry feature that spells "JPL" in Morse code.

Figure 3. Primary features of the MSL wheel. Image Credit: NASA/JPL-Caltech

six titanium flexures (spokes) that also function as suspension springs [4]. Figures 2 and 3 illustrate the sections and features of the MSL wheel.

The MPF wheel body, MER wheel, and MSL wheel are constructed of aluminum for its high strength-to-weight ratio. Several factors put MSL wheels at a higher risk of damage than MPF and MER.

1. Curiosity has a significantly larger mass than MPF (78.17x) and MER (4.86x), which translates into larger load bearing forces on its wheels.
2. Curiosity's wheels are nearly four times as tall as MPF wheels and twice as tall as MER wheels, enabling them to climb over taller rocks, which translates into longer contact times with rocks and larger wheel drops off of rocks.
3. Curiosity's wheels have fewer grousers than MER wheels, which translates into a larger distance between grousers and more opportunities for rock features to contact and damage wheel skin.
4. Curiosity's wheels have thinner skin than MER wheels (0.75 mm vs. 3.52 mm), making them more susceptible to skin punctures.

The decision to use 0.75 mm wheel skin for MSL's wheels, the absolute minimum thickness that was machinable, was a consequence of the need to minimize both the total mass of the rover and also the loads experienced by the suspension system when it is deployed during the Entry-Descent-Landing (EDL) phase of the mission. While the MSL wheels were designed to operate with considerable damage, the rate at which damage was occurring was unexpected and raised concerns regarding wheel life expectancy and the ability to meet the mission goal of performing science over at least 20 km of odometry.

In December 2013, a multi-institution Tiger team of 13 individuals with expertise in geology, mechanical system engineering, failure analysis, rover operations, mobility performance, stress analysis, ADAMS analysis, and materials was formed to determine the cause of the excessive wheel wear and to recommend a strategy to reduce the wheel damage rate. Extensive characterization of the mechanism of wheel damage per terrain type is described in [5] and [6] and summarized in [7]. In general, the high wheel damage rate was attributed to a combination of driving over pointed, embedded rocks not seen at previous Mars rover landing sites, and the use of a motor control algorithm that drove each wheel at the same speed, irrespective of wheel/terrain interaction. To reduce the rate of wheel damage, a terrain-adaptive wheel speed control software patch called TRCTL was developed and installed on Curiosity [8].

The size of cracks in wheel skin can grow over time, increasing the loading on nearby grousers. Wheel life-cycle testing in the JPL Mars Yard showed that a grouser is at risk of breaking once at least 70% of the skin between the wheel's inner edge and the stiffener ring is cracked on both sides of the grouser. Periodic imaging of the wheels and a method for quantifying and tracking the damage level of each wheel was implemented.

Wheel damage inspection images are acquired by the Mars Hand Lens Imager (MAHLI), an instrument mounted on the turret on the end of the robotic arm. Supplemental wheel damage inspection images of the right wheels are also acquired by the Mast Camera (Mastcam), which is mounted on the Remote Sensing Mast (RSM). Single position MAHLI wheel imaging (SPMWI) sequencing was developed to acquire an image of each wheel in a single wheel position. Full MAHLI wheel imaging (FMWI) sequencing was developed to acquire an image of each wheel in five equal-distance wheel positions.

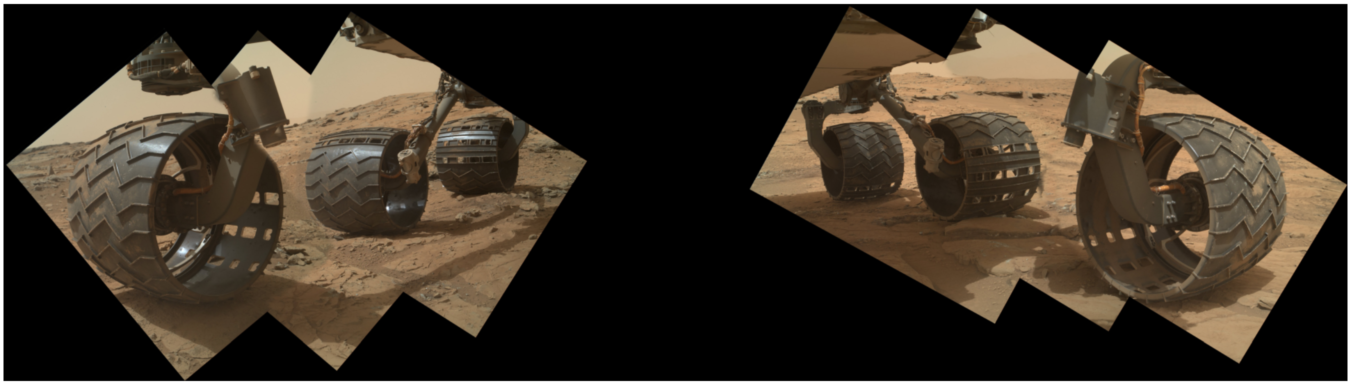

Figure 4. Mosaic of the six MAHLI wheel images acquired on sol 177. Image Credit: NASA/JPL-Caltech

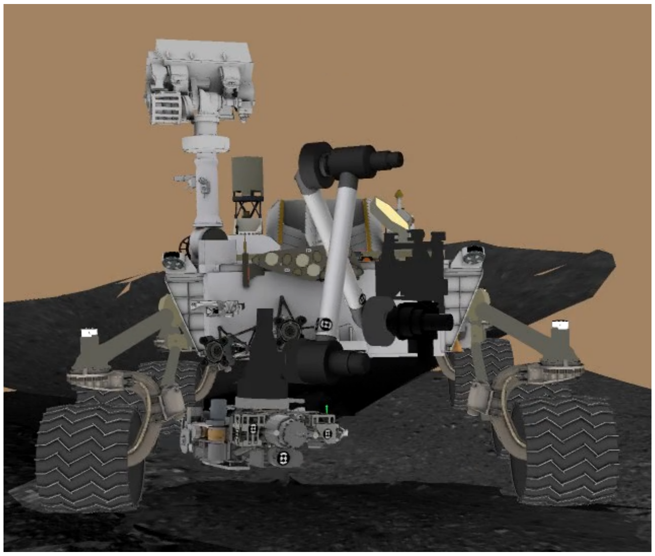

Figure 5. A frame from the sol 2030 underbelly FMWI animation generated during uplink planning.

Figure 6. Cropped sol 34 MAHLI image of the LM wheel showing the first observed damage to Curiosity wheels. Image Credit: NASA/JPL-Caltech

Wheel damage assessment is primarily performed with FMWI after driving a specified number of meters. The first FMWI was completed on sol 490. Since then, the FMWI frequency has been adjusted several times and is currently executed every kilometer. After each FMWI, wheel damage is assessed by measuring each individual crack in wheel images and tabulating the cumulative crack length within each skin section and the cumulative crack length for each wheel, denoted left front (LF), left middle (LM), left rear (LR), right front (RF), right middle (RM), and right rear (RR). SPMWI provides a snapshot of a portion of each wheel at a less uniform cadence and is used to identify significant changes in damage level, but not to measure crack lengths.

As of sol 3150, Curiosity has three broken grousers on the LM wheel and one broken grouser on the RM wheel. Changes in the damage growth rate have influenced the wheel imaging frequency, the method of damage tracking, and driving guidelines throughout Curiosity's mission. In this paper we describe wheel imaging, the process for assessing wheel damage and how it has evolved over time, the current state of Curiosity's wheels, and how the damage assessment has influenced driving methods and restrictions.

2. Wheel Imaging

Prior to launch, cracks had been observed in MSL wheels on a testbed rover. Therefore, early in the mission, the Operations team periodically performed SPMWI to monitor the health of the wheels. The first and second SPMWI were performed on sol 34 and 177, after 108.9 m and 723.4 m cumulative odometry, respectively. A sequence was executed that moved the robotic arm into a configuration that positioned the MAHLI to point under the belly of the rover to acquire images of each wheel. Figure 4 shows a mosaic of the six sol 177 MAHLI wheel images and Figure 5 illustrates the arm configuration for underbelly wheel imaging.

The first Curiosity wheel damage was discovered during an inspection of the sol 34 MAHLI image of the LM wheel. As shown in Figure 6, light could be seen shining through a crack in the LM wheel skin, as observed from the underside of the wheel. The Tiger team concluded that this crack is likely from wheel/terrain interaction during Curiosity's touchdown on the surface of Mars.

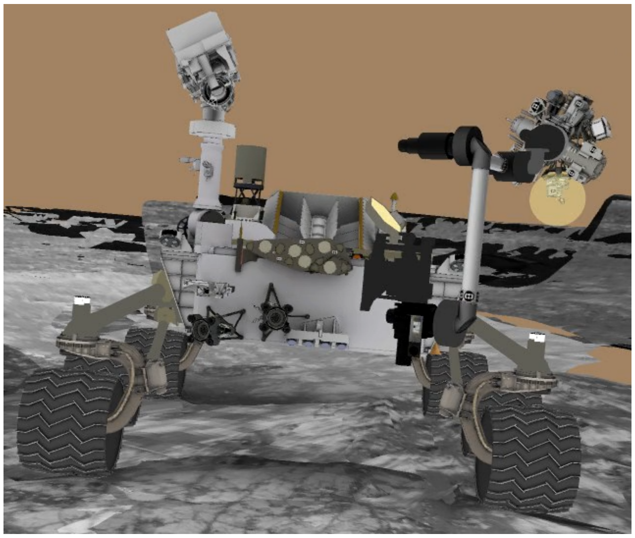

Figure 7. A frame from the sol 2115 overhead FMWI animation generated during uplink planning.

In the sol 275 SPMWI (after 727.2 m), a few pin hole punctures were observed in several wheels. More concerning, in the sol 463 SPMWI (after 4,420.2 m cumulative odometry), medium-sized holes were observed in the LF and LM wheels. The SPMWI frequency guideline was then increased to every 50 m. Six sols later (on sol 469), another SPMWI was performed and several cracks were observed in the RM, LM, and LF wheels. After three more SPMWI (on sols 472, 476, and 486), Curiosity started its first FMWI on sol 488 and completed it on sol 490.

FMWI enables wheel damage characterization over the full surface of the six wheels. MAHLI and Mastcam take images of each wheel, then the rover drives forward to rotate the wheels. The cameras image the newly exposed sections, and the process is repeated until all wheels rotate one revolution for full coverage. The arm must be stowed during driving to protect it from impacting terrain and experiencing terrain induced shock while extended. Therefore, the arm is stowed prior to executing each FMWI drive step and unstowed after for imaging. During FMWI drive steps, visual odometry is enabled to document wheel slippage. TRCTL is not used for FMWI driving so that each wheel rotates the same amount during each drive step, regardless of the terrain shape.

For the first two FMWI (sols 488+490 and 512+513+515), the drive distance between acquiring sets of wheel images was 0.262 m, which corresponds to a wheel rotation of 60°. Wheel imaging was performed before the first drive step and after each of five drive steps over a total drive distance of 1.31 m. Starting with the sol 521 FMWI, the drive distance between acquiring sets of wheel images has been 0.314 m, which corresponds to a wheel rotation of 72°. Wheel imaging is performed before the first drive step and after each of four drive steps over a total drive distance of 1.256 m.

Starting on sol 587, the number of MAHLI images acquired at every wheel position was reduced from six to four, decreasing the overall number of MAHLI wheel images needing to be downlinked each FMWI from 30 to 20. Two MAHLI images of the middle wheels were identified as redundant given the images of the rear wheels also have the middle wheels in the frame. The redundant images were removed from the imaging sequence.

By sol 2113, Curiosity had driven 600.5 m since the previous FMWI and was 100 m overdue for a FMWI. However, there was a dust storm in the vicinity of Curiosity and there was concern about dust collecting on the MAHLI lens during a FMWI. On sol 2114, a set of MAHLI wheel images were captured with the MAHLI lens cover closed, but analysis by the mobility team deemed the quality of the images insufficient for performing wheel damage assessment.

On sol 2115, a change was made to acquire overhead MAHLI wheel images instead of underbelly MAHLI wheel images. The MAHLI pointing during overhead wheel imaging is closer to nadir than during underbelly wheel imaging, decreasing the risk of dust accumulating on the lens while the lens cover is open. Figure 7 illustrates the arm configuration for acquiring overhead MAHLI wheel images.

Because the base of the arm is on the left side of the rover, only the left wheels and RF wheel can be imaged with the MAHLI from an overhead arm configuration. Similarly, because the RSM is mounted on the right side of the rover, only the right wheels can be imaged by the Mastcam. Since sol 2115, wheel damage assessment has been performed using overhead MAHLI wheel images to assess the left wheels and the RF wheel, and Mastcam wheel images to assess the RM and RR wheels.

The RM wheel is the closest wheel to the RSM and cannot be fully imaged by the Mastcam using a single pointing angle. Therefore, at each wheel position, two Mastcam images are acquired of the RM wheel using slightly different RSM pointing angles. Figure 8 illustrates the three Mastcam wheel images and Figure 9 illustrates the four overhead MAHLI wheel images. In the images of the rear wheels, a portion of the wheels are occluded by the bogie suspension arms. This is acceptable for wheel damage assessment since the rear wheels currently have insignificant damage.

MAHLI and Mastcam wheel images are captured at a resolution of 1632x1200 and 1408x1200 pixels, respectively. On FMWI sols, Rover Planners (RPs) build a drive sequence that includes FMWI commands. Additional driving is sometimes included in the drive sequence after the FMWI activities. On sol 3195, the duration of the FMWI portion of the drive sequence was 117.7 minutes.

The plot in Figure 10 illustrates the period of increased SPMWI frequency and start of FMWI after a medium size hole was observed in the LF and LM wheels on sol 463. A FMWI event is often completed in a single sol, but it also has been common to complete it over two or more sols. On sol 1269, two SPMWI events were performed in part to image the terrain under the RR wheel following a RR drive actuator stall on sol 1267. Since sol 2407, all of the FMWI events have been performed on a single sol.

Figure 11 illustrates that post SPMWI or FMWI driving can be planned. Post SPMWI and FMWI driving was common around sol 500-750. During that period, there were three drives after MAHLI wheel imaging that exceeded 100 m. Figure 12 illustrates what the cumulative odometry was prior to each MAHLI wheel imaging event.

Figure 8. The three sol 3195 Mastcam wheel images. Image Credit: NASA/JPL-Caltech

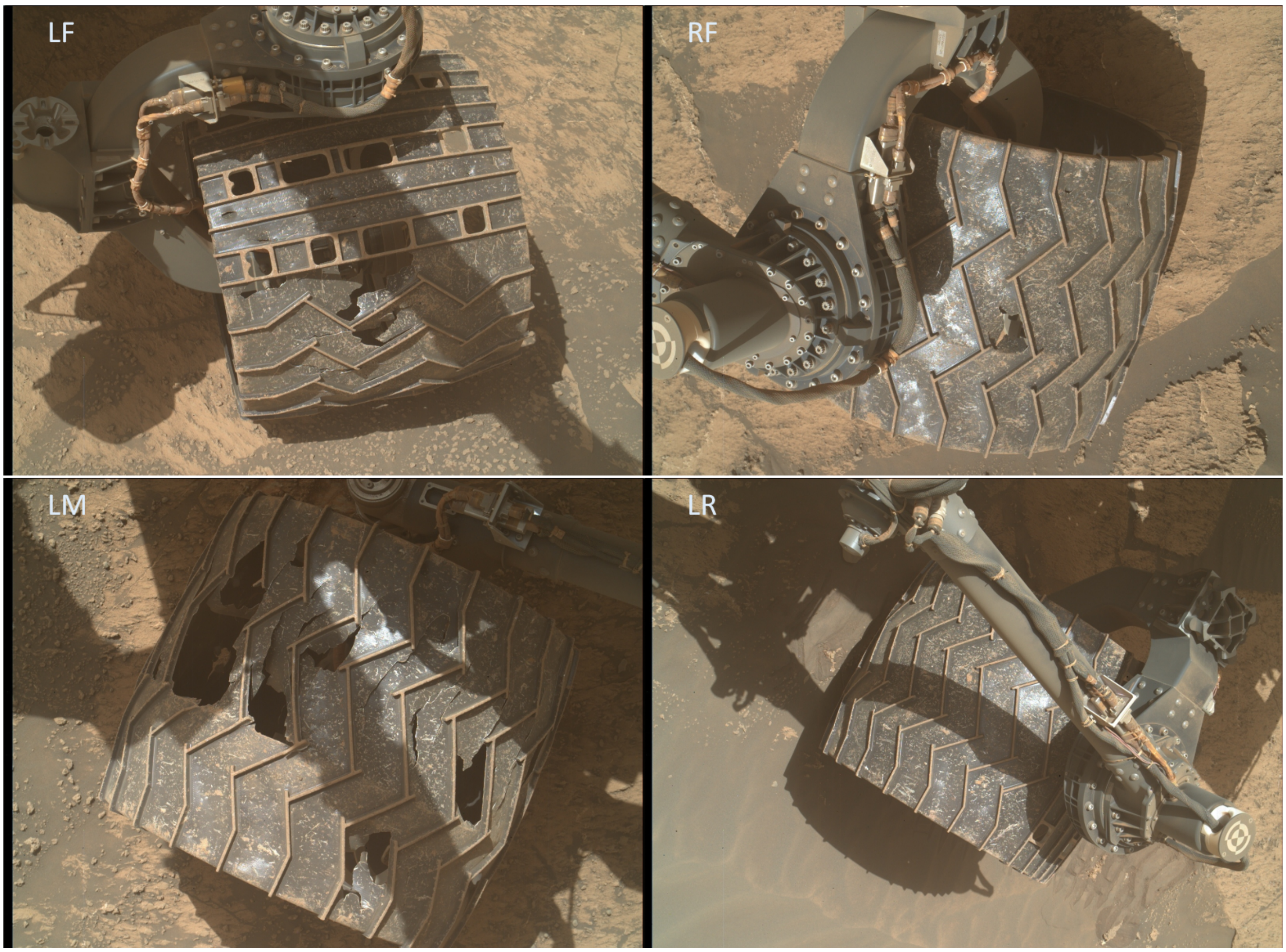

Figure 9. The four sol 3195 MAHLI wheel images. Image Credit: NASA/JPL-Caltech

3. Process for Assessing Wheel Damage

Curiosity wheel damage assessment is performed by the MSL Wheel Wear team, which is a subset of the MSL Mobility Operations team. The wheel damage assessment process has several evaluations of increasing detail at each stage.

1. Tactical assessment (15 minutes)
2. Initial look assessment (1 day)
3. Crack length measurement (1-2 weeks)

Tactical operations involves assessing rover health and safety from the most recent downlinked data, and generating and reviewing next-sol sequences prior to a pre-scheduled uplink window. The tactical and initial look assessments are qualitative evaluations focused on identifying major changes that may impact tactical operations. For example, discovery of a significant change in wheel state may lead to changes in sol plans or constraints. Tactical and initial look assessments are followed by measurements of the cracks (damage features) to quantify wheel damage. The measurements are compiled with historical data for long term trending.

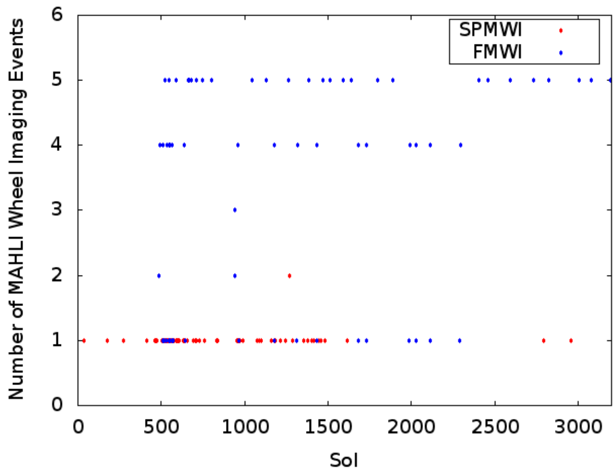

Figure 10. MAHLI wheel imaging events per sol.

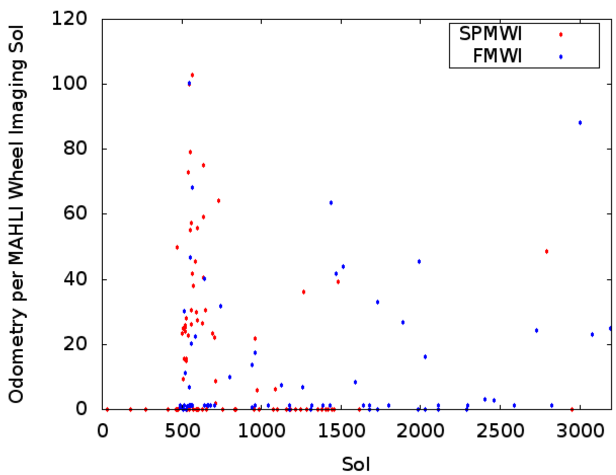

Figure 11. Total odometry achieved on each sol MAHLI wheel imaging was performed.

When a new set of FMWI images is received, a mobility downlink analyst checks for any major changes in wheel damage during the next tactical shift. Images are compared to the previous set for new grouser breaks, new damage features, large growth in existing features, and other off-nominal changes such as rocks stuck within wheel holes. This tactical assessment usually takes less than 15 minutes and is focused on identifying changes in wheel state that may restrict activities that can be planned for the next sol. The six wheels are then divided across the Wheel Wear team for more detailed assessments. Each member is assigned one or two wheels on a rotating basis to reduce assessor bias.

For the initial look assessment, each wheel is evaluated in detail for qualitative changes. Current images are compared with those from the previous FMWI set to identify grouser breaks, new features, and existing features that grew or merged. The Wheel Wear team discusses initial look findings to establish consensus on the states of the wheels, and to determine if additional analysis is required. The initial look assessment is generally performed in less than one day.

An example is the identification of a large skin flap protruding into the LM wheel, first seen in MAHLI images on sol 1127.

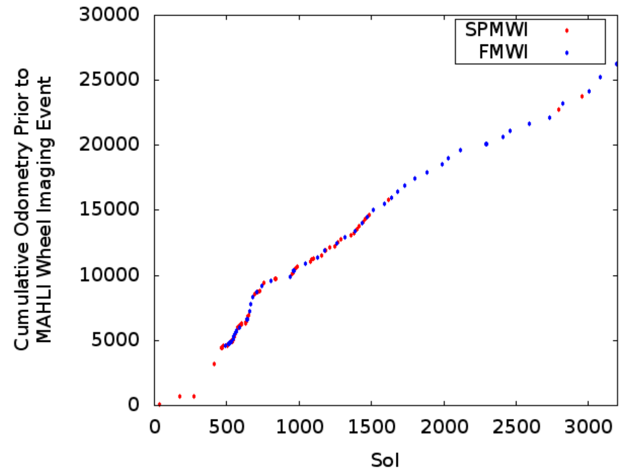

Figure 12. Cumulative odometry prior to each MAHLI wheel imaging event.

It required analysis to determine the risk to the LM wheel actuator's cable bundle. The Wheel Wear team agreed that it was not long enough to be an immediate hazard, and since the base of it was a grouser, it could not grow any longer. The risks from skin flaps are discussed in Section 4 and the large skin flap on the LM wheel is illustrated in Figure 27.

After completing the qualitative assessments, the cracks on the wheels are measured. Each wheel has a crack map that shows the locations and shapes of the features on it. The LM wheel crack map is illustrated in Figure 13. Cracks are numbered in order of their discovery (larger numbers are the most recent). The size of each crack is expressed in terms of a dimensionless ratio by dividing the length of a crack along the width of the skin section, by the width of the skin section. This is done by taking a pixel measurement of the skin section that a crack is on, and a pixel measurement of the crack length parallel to the previous measurement. As illustrated in Figure 14, an image manipulation tool such as GNU Image Manipulation Program (GIMP) is used to take pixel measurements.

The measurements are compiled in a spreadsheet to track long-term trends. The spreadsheet has logic to accommodate cracks that could not be measured due to lighting conditions, and for cracks that merge together. It provides the data for other trending tools such as a crack length analysis dashboard (Figure 22) that summarizes the conditions of the wheels, and the life model for comparison with Mars Yard three-wheel test track data (Figure 29).

Due to the changes in conditions between FMWI sets, the measurement process is manually intensive. Sunlight may highlight particular features on a given sol more than previously seen and completely obscure others. The wheel positions are not consistent between FMWI sets so assessors must visually orient themselves based on the wheel grousers and damage features, especially where only the non-odometry grousers are visible. This process of correlating 2D representations of 3D features to 2D imagery in inconsistent conditions results in measurement variance.

Figure 15 and Table 2 show the variability between measurements of each crack, grouped by wheel. The front and middle wheels have tight distributions with average differences an

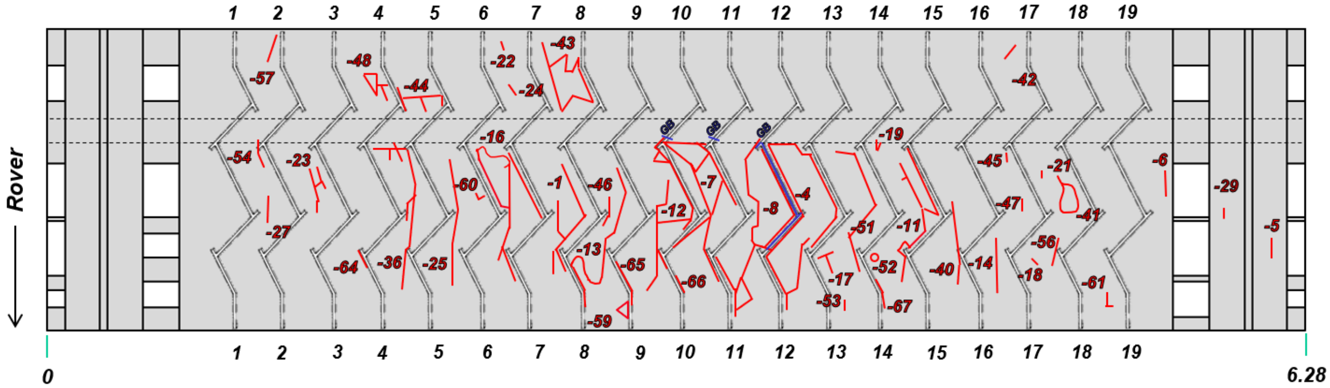

Figure 13. Sol 3195 LM wheel crack map. Image Credit: NASA/JPL-Caltech

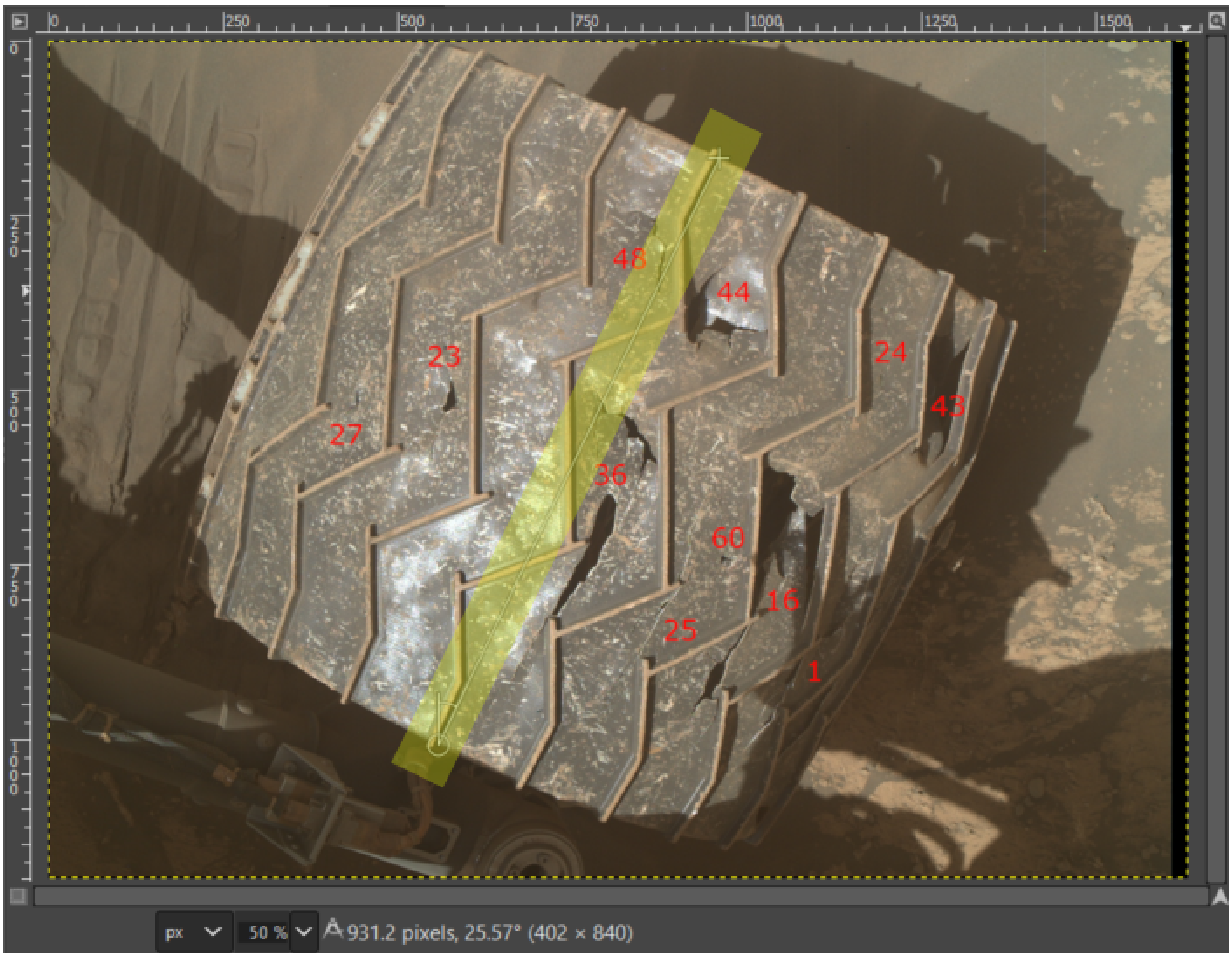

Figure 14. Sol 3195 pixel measurement of the LM wheel using GIMP. Image Credit: NASA/JPL-Caltech

order of magnitude smaller than the average crack measurement. The larger spread for the two rear wheels is due to the low sample size from not having accumulated as much damage. Numbers in the "Overall" row in Table 2 are the average length and average differences of all cracks on all wheels. The data shows that variances between a crack's measurements are minor relative to the width of the wheel, with the overall average difference between measurements of all wheels being just 1.498 mm compared to the wheel width of 400 mm. The rear wheels have fewer and smaller damage features than the middle and front wheels. This combined with a reduced resolution from being further away in wheel images results in fewer measurements made throughout the mission and contributes to the larger measurement error seen on the LR and RR wheels.

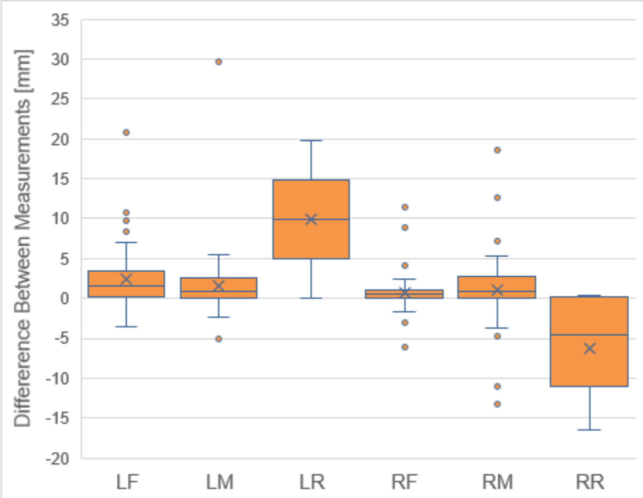

Figure 15. Variability between measurements of cracks, by wheel.

Table 2. Summary of Crack Measurements

Wheel	Average Crack Length Measurement [mm]	Average Difference Between Measurements [mm]	Number of Measurement Samples
LF	35.546	2.348	1208
LM	43.639	1.611	1144
LR	22.203	9.931	4
RF	16.582	0.740	472
RM	36.518	1.083	1559
RR	22.524	-5.048	19
Overall	35.011	1.498	4406

4. Current State of Curiosity's Wheels

The current state of Curiosity's wheels is best understood when put in context with the progression of wheel wear over the course of the mission. Key wheel wear events are listed in Table 3.

On sol 490, the first FMWI was completed after the first sizeable holes on the rover wheels were observed. Following this event, a Tiger team was formed that conducted extensive testing and algorithm development to reduce the wheel damage rate. A significant event in the life of each wheel is when grouser breaks are first discovered. By sol 3195, the Wheel Wear team had discovered three grouser breaks on the LM wheel and one grouser break on the RM wheel. The first two grouser breaks on the LM wheel were discovered in sol 1641 wheel images and the 3rd grouser break on the LM wheel was discovered in sol 3079 wheel images.

TRCTL was approved for nominal use in flight on sol 1678, following the discovery of the first two LM grouser breaks in sol 1641 wheel images. Since then, the wheel grouser break rate has been significantly slower than predicted by the Tiger team. However, while there have been decreases in damage rates, it is challenging to distinguish if they are due to TRCTL or driving over easier terrain. The first and only grouser break on the RM wheel was discovered in sol 2407 Mastcam wheel images.

Table 3. Key wheel wear events

Sol	Event
34	The first SPMWI. First wheel damage observed (a crack on the LM wheel)
490	The first FMWI was performed after sizeable holes were observed on sol 463
516	Restriction against use of Autonomous navigation (AutoNav) and multi-sol drives started
1641	Two grouser breaks discovered on the LM wheel (grousers 10 and 12)
1678	TRCTL was approved for nominal use in flight
1781	AutoNav is once again permitted in all terrain types when conditions warrant it
2407	First grouser break discovered on the RM wheel (grouser 12)
3079	Third grouser break discovered on the LM wheel (grouser 11)
3195	Latest FMWI (downlinked August 2, 2021)

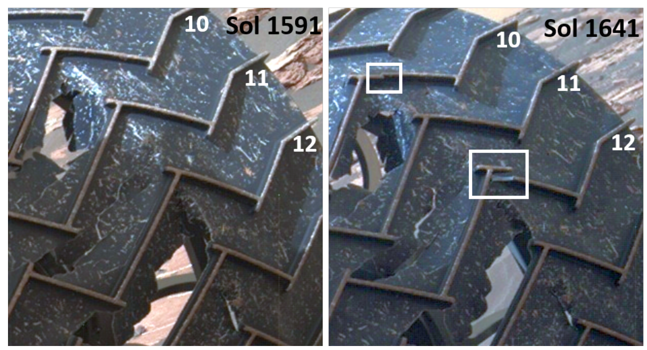

Figure 16. A break occurred on grousers 10 and 12 of the LM wheel sometime between sol 1591 and 1641.

On sol 2115, the Operations team implemented overhead capturing of MAHLI wheel images, which resulted in more detailed documentation of the wheel state. The current status of Curiosity's wheels is based on the latest FMWI performed on sol 3195, from which the Wheel Wear team concluded that maintaining a cadence of conducting FMWI every 1 km is sufficient for monitoring wheel damage.

According to Tiger team guidelines, three grouser breaks on a single wheel is considered a milestone that requires reevaluation of the current driving and wheel imaging guidelines. After the sol 3079 FMWI, when the 3rd grouser break on the LM wheel was documented, the Wheel Wear team concluded that based on the rate of damage observed over the past few FMWI, the 3rd grouser break should not be alarming and the current guidelines for driving are effective for reducing wheel damage. Figures 16, 17 and 18 illustrate the progression of grouser breaks on the LM wheel.

Figure 16 shows the state of LM wheel grousers 10, 11, and 12 on sol 1591, before any grouser breaks had been discovered, and on sol 1641, when the grouser 10 and 12 breaks were discovered. In the sol 1641 image, there is obvious separation where the grouser 12 break occurred, but the grouser 10 break is subtle, not detected by a clear

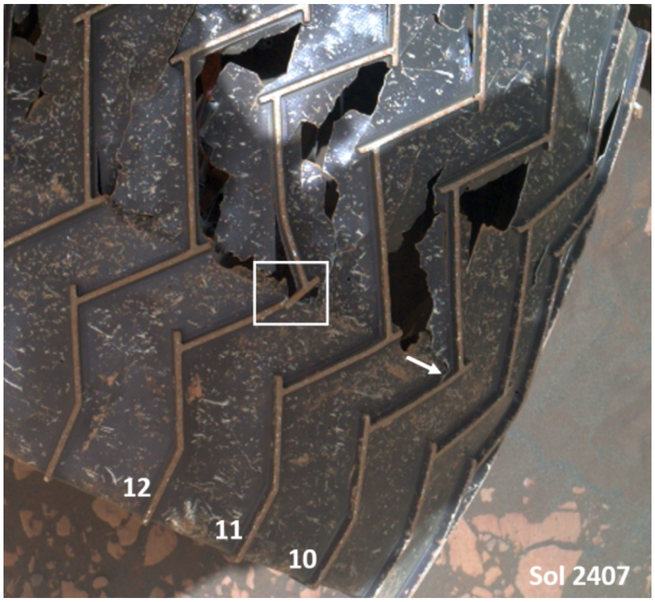

Figure 17. Status of the grouser 10 and 12 breaks on the LM wheel on sol 2407.

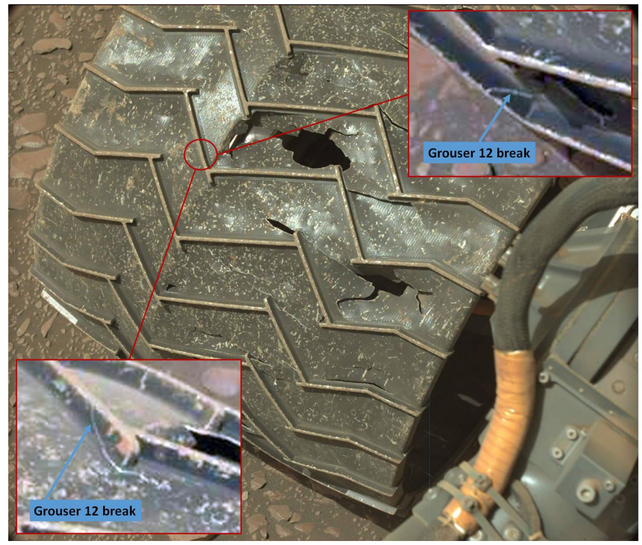

Figure 19. A view of the grouser 12 break on the RM wheel on sol 2407. The grouser break is not observable from a top-down view, but can be clearly seen from views of both sides of grouser 12.

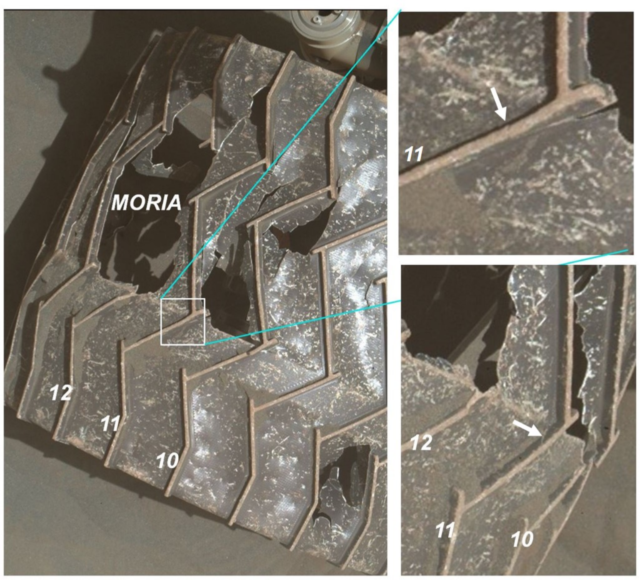

Figure 18. A view of the grouser 10, 11, and 12 breaks on the LM wheel on sol 3079. The grouser 11 break is observable from a top-down and side view.

separation but by a slight misalignment in the top-down view of the grouser.

Figure 17 shows the state of LM wheel grouser breaks 10 and 12 on sol 2407. At the grouser 12 break, there is much less lateral separation than previously seen on sol 1641 and a visible lateral bend in grouser 12. At the grouser 10 break, there is no visible separation or misalignment, but the crack from the base to the top of the grouser is visible from a side view of the grouser.

Figure 18 shows the 3rd grouser break (on grouser number 11) on the LM wheel, discovered on sol 3079. The break is slightly visible in a top-down view and confirmed in a side view. The biggest damage feature on the LM wheel is named Moria (named after the Dwarven city from J.R.R. Tolkien's works, and voted for by the MSL team). As illustrated in Figure 19, the only grouser break on the RM wheel (on grouser number 12) is not visible from a top-down view of the grouser, but is visible from views of each side of the grouser.

Figures 20 and 21 show wheel status per skin section and cumulative damage per wheel section, respectively, for the front and middle wheels on sols 490, 1682, and 2115. There was a significant increase in wheel damage from sol 490 to 1682 and a relatively small increase from sol 1682 to 2115. The red lines in Figure 20 are the broken grousers and blue lines are the at-risk grouser due to high damage in the skin section around them. The yellow skin sections in Figure 20 are ones with some damage and orange skin sections are ones with significant damage. The green sections in Figure 20 are the wheel sections with minimal damage.

The percentage of wheel damage per skin section can be seen in Figure 21. The damage on the RR and LR wheels is not depicted in the figures; this is due to the minimal damage these wheels have experienced. The relatively low damage on the LR and RR wheels is illustrated in Figure 22.

After 26,255 m of driving on Mars (as of sol 3195), damage to Curiosity's wheels is less severe than predicted by the Tiger team (see Section 5). The number of grouser breaks is less than what the Tiger team expected by this amount of total odometry, and the Wheel Wear team has observed a relatively slow increase in wheel damage. Table 4 shows the number of features on each wheel, and the cumulative crack length for each wheel is shown in Table 5.

Table 4. Number of features on each wheel.

	Left	**Right**
Front	60	33
Middle	44	64
Rear	2	5

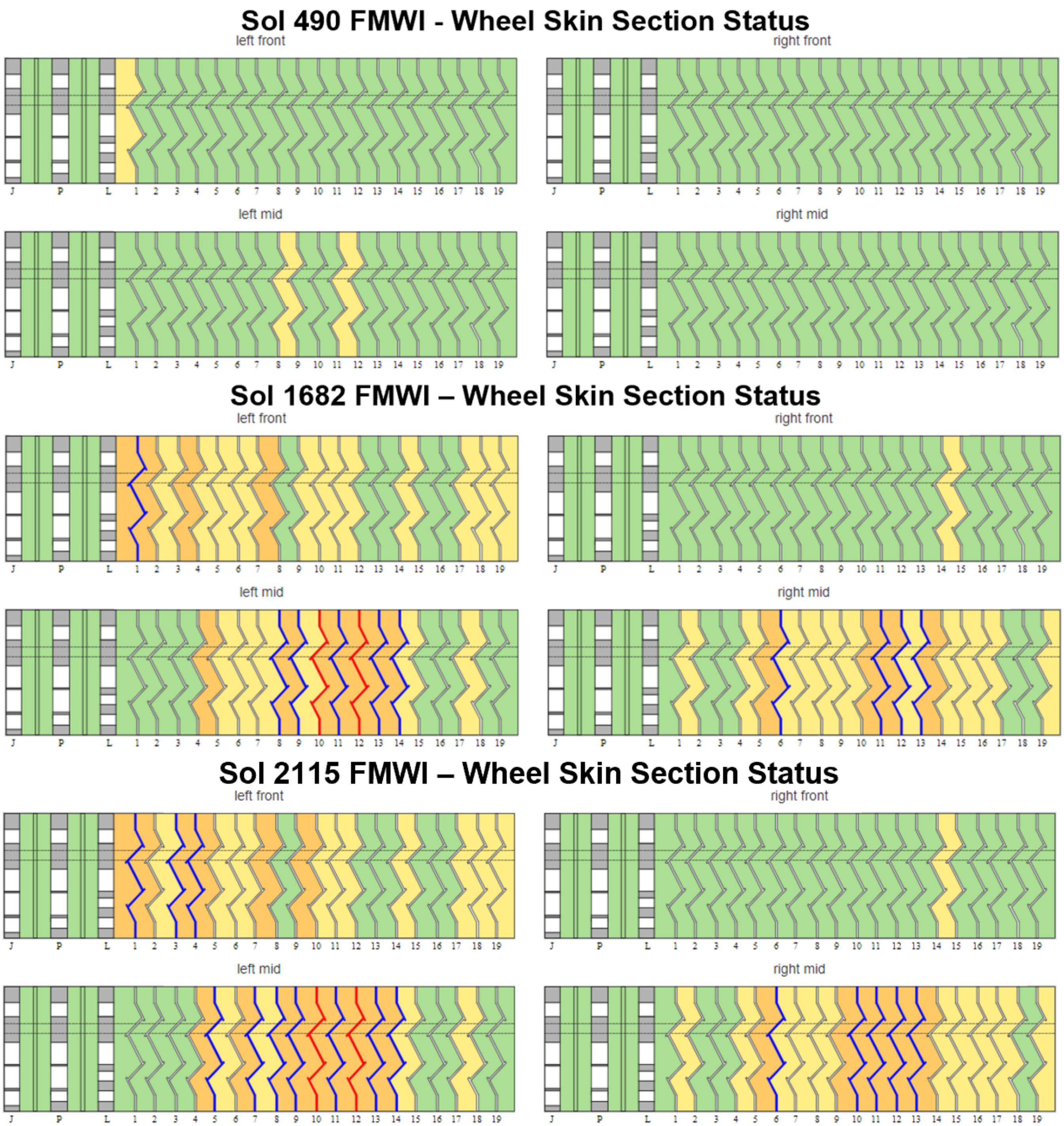

Figure 20. Damage per wheel skin sections for sols 490, 1682 and 2115

Table 5. Cumulative crack length of each wheel (mm).

	Left	Right
Front	3,341	772
Middle	2,950	3,466
Rear	65	129

The RM wheel has the most features and largest cumulative crack length, followed by the LF wheel and then the LM wheel. The LF wheel has nearly twice as many features and 4.3 times the cumulative crack length as the RF wheel. There is no obvious explanation for the disparity in damage between the LF and RF wheel, and although there are several hypotheses, this subject is still under investigation.

Figure 22 shows wheel status per skin section and cumulative damage per wheel section, as of sol 3195. Figures 23, 24, 25 and 26 contain all the front and middle wheel images acquired during the sol 3195 FMWI, with some notable features annotated by their identification numbers.

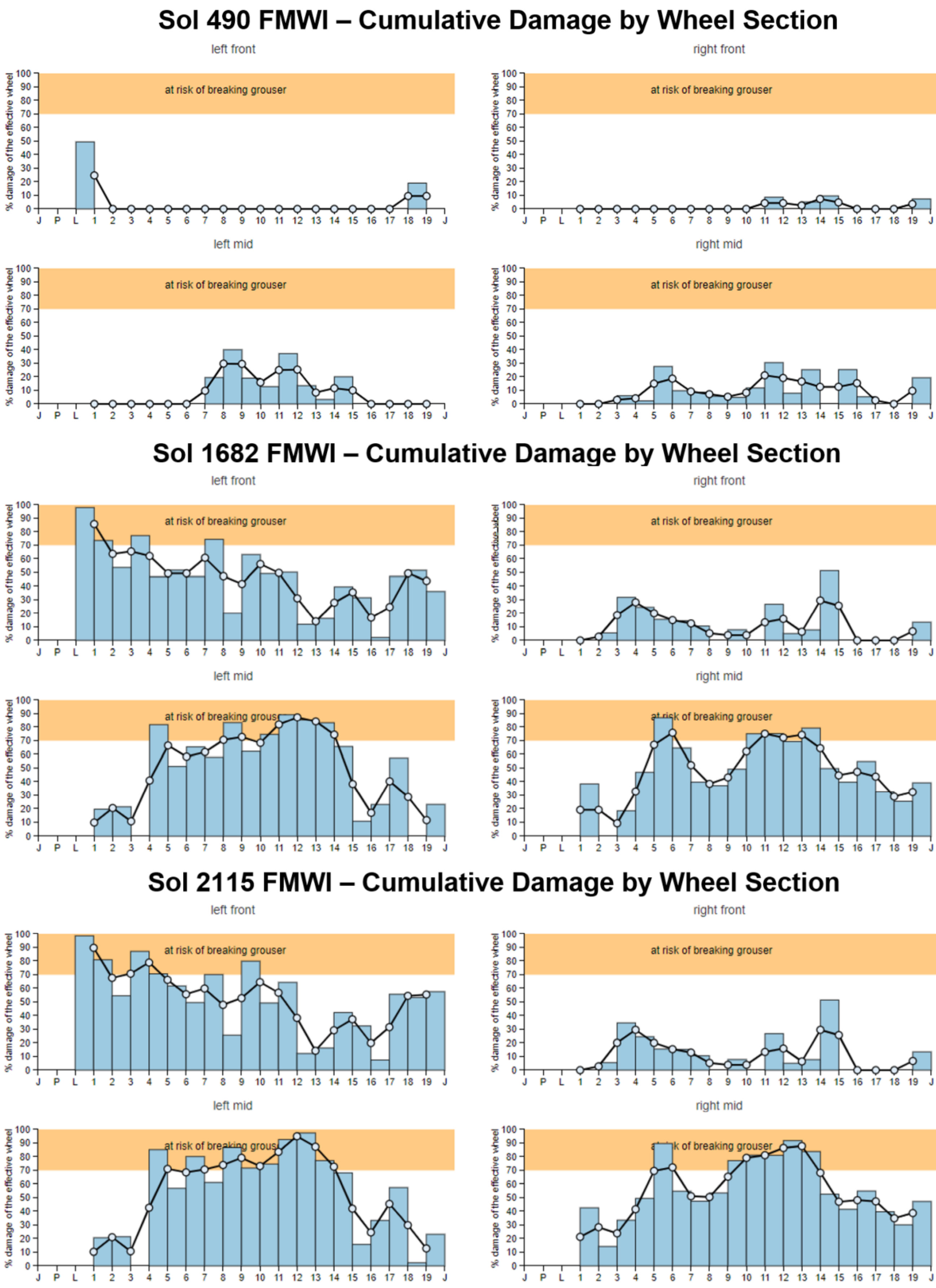

Figure 21. Cumulative damage per wheel sections for sol 490, 1682 and 2115.

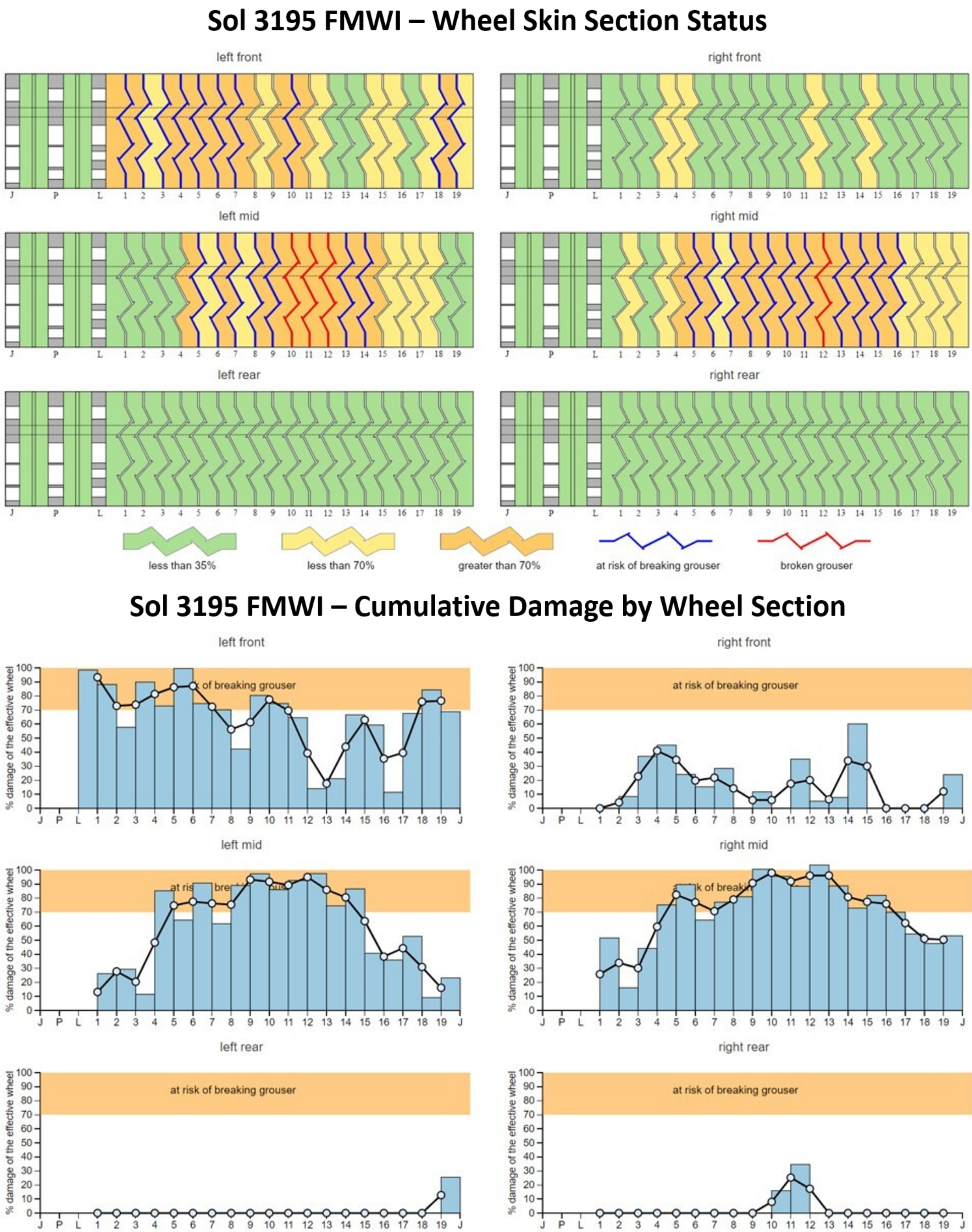

Figure 22. Wheel skin section status and cumulative damage per wheel sections, as of sol 3195

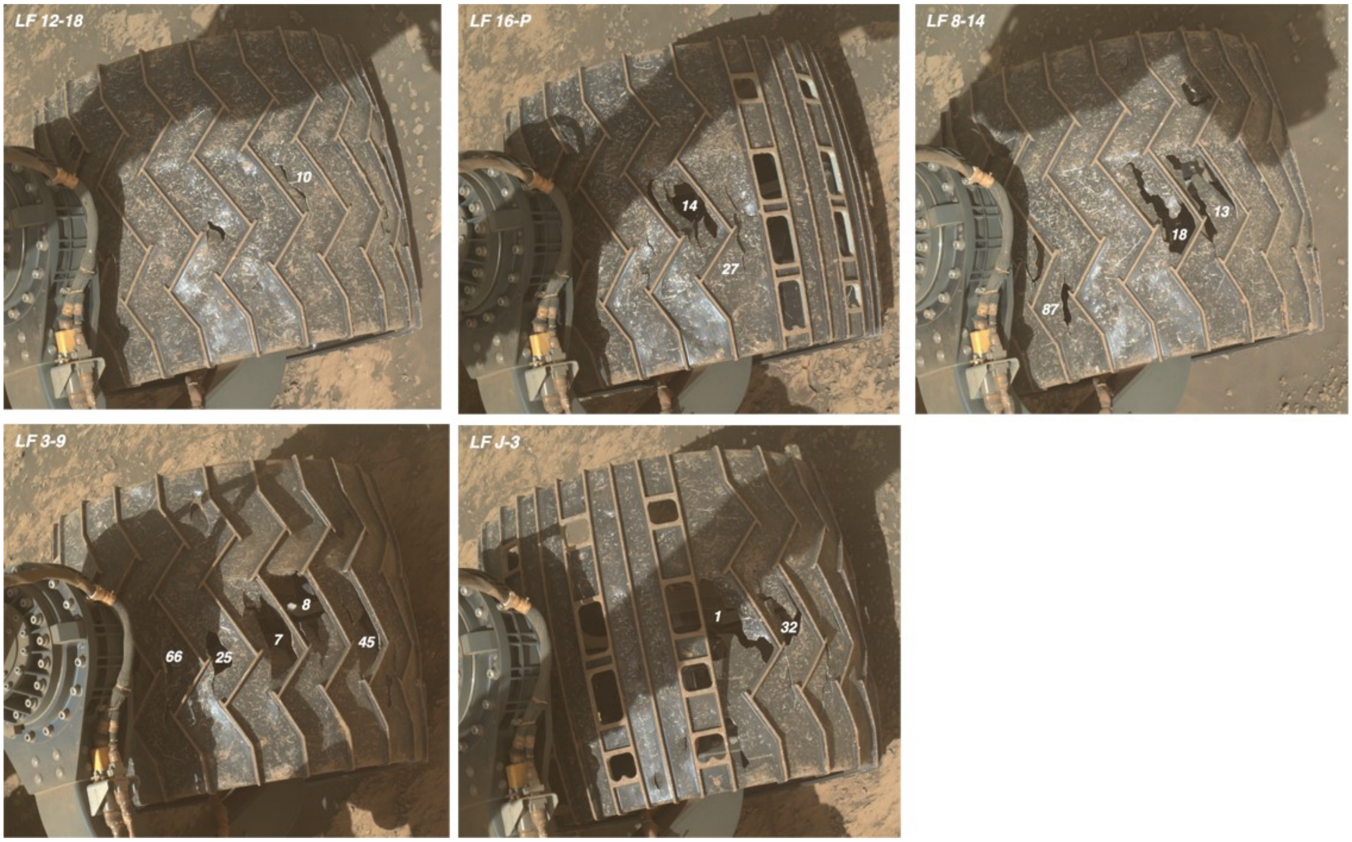

Figure 23. Sol 3195 MAHLI images of the LF wheel. Image Credit: NASA/JPL-Caltech

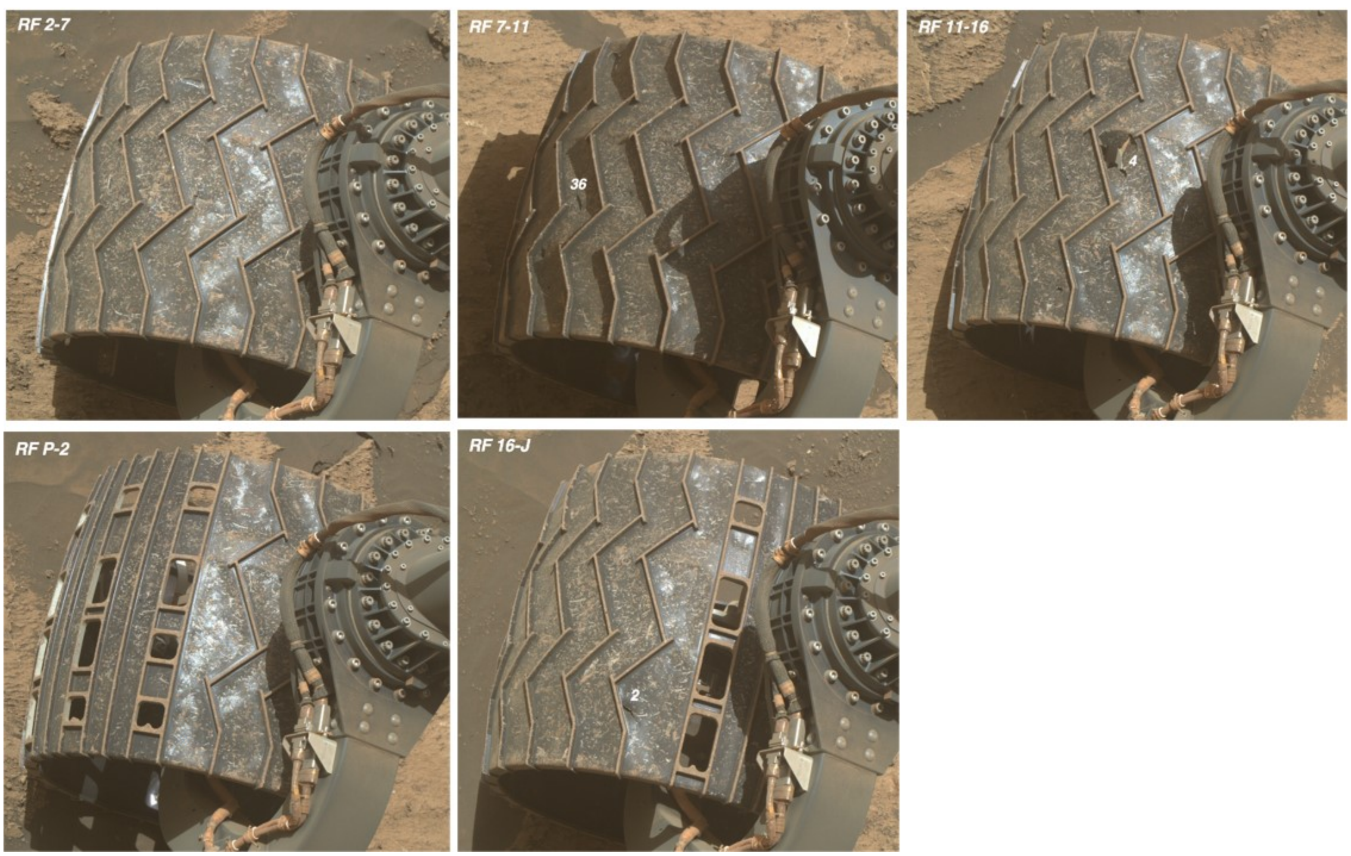

Figure 24. Sol 3195 MAHLI images of the RF wheel. Image Credit: NASA/JPL-Caltech

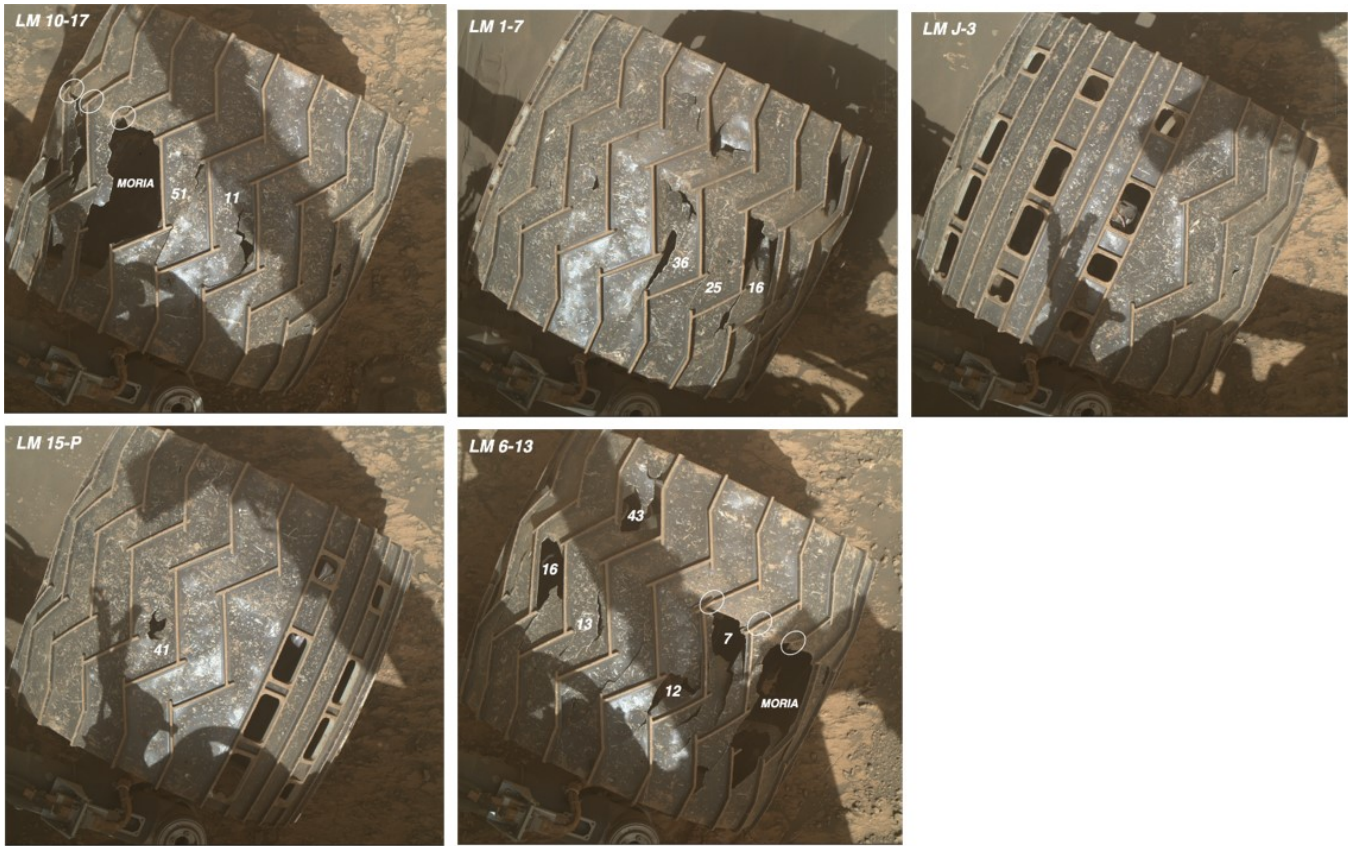

Figure 25. Sol 3195 MAHLI images of the LM wheel. Image Credit: NASA/JPL-Caltech

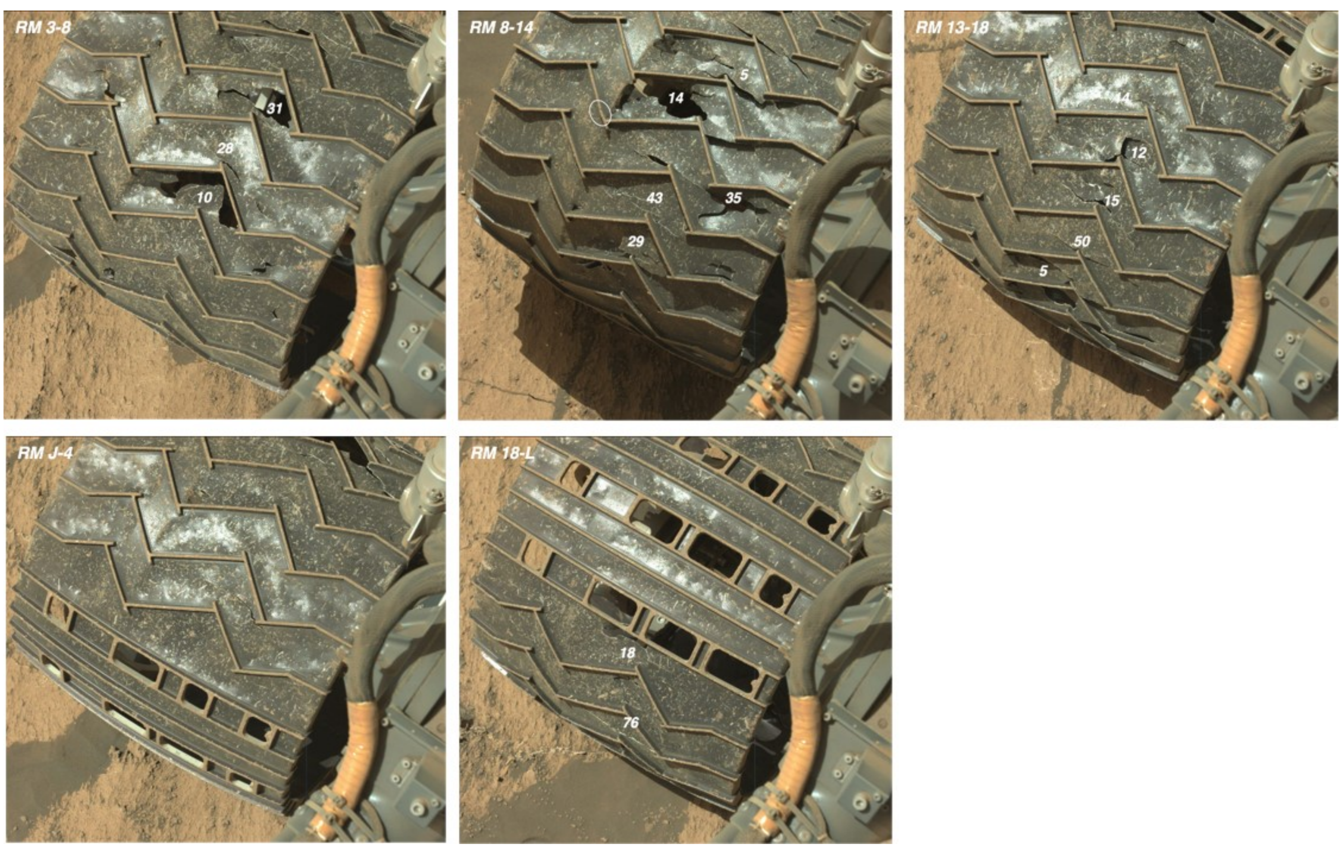

Figure 26. Sol 3195 Mastcam images of the RM wheel. Image Credit: NASA/JPL-Caltech

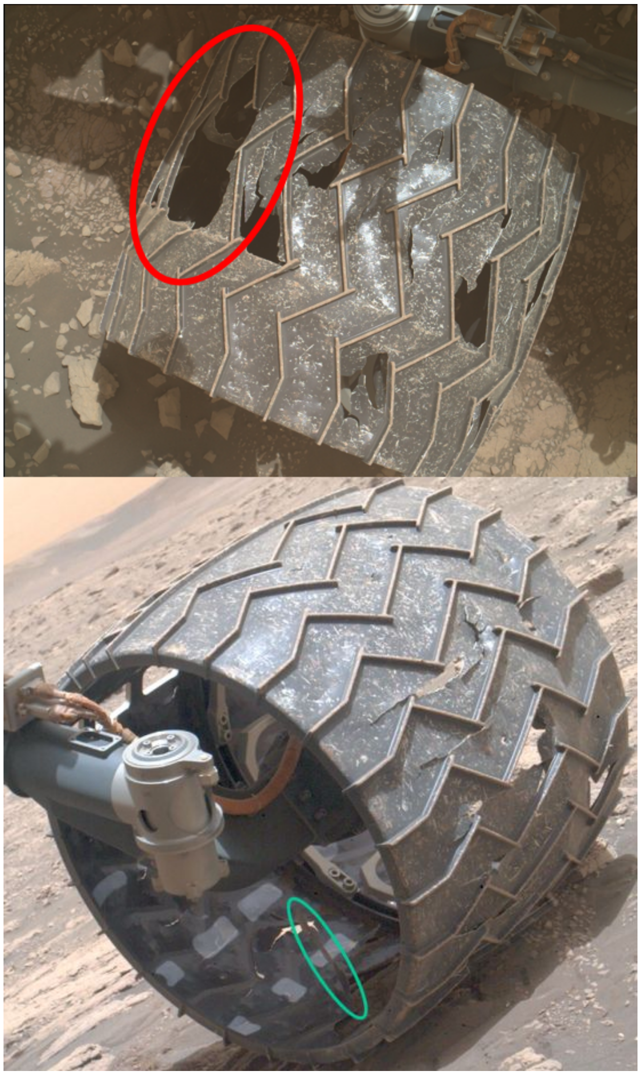

Figure 27. Sol 3005 overhead MAHLI view (top) and sol 3011 underbelly MAHLI view (bottom) of a flap of skin bent inward on the LM wheel inbetween grousers 12 and 13.

Where there is a large hole in a wheel, a skin section has either broken away from the wheel and fallen onto the Martian surface or the skin section is still attached to the wheel and is pushed inward. A skin section that is still attached to the wheel and pushed inward is called a flap. A flap is identified by the wheel it is on and the crack number it is associated with. Figure 27 shows an overhead and underbelly MAHLI view of flap LM-4, acquired on sol 3005 and 3011, respectively. Flap LM-4 is in between grouser 12 and 13 and was first observed in the sol 1127 FMWI.

Theoretically, a flap could be long enough to contact the cable that runs to a wheel actuator. Damage to a wheel actuator cable could cause loss of commandability of that wheel. Therefore, flaps are monitored each FMWI. However, the risk of a flap causing damage to a wheel actuator cable is considered low. Finite element analysis indicates that a flap of wheel skin long enough to reach a wheel actuator cable would break off before contacting a cable.

The length of flap LM-4 is estimated to be 109.8 mm, well short of the 181.5 mm minimum distance between the inner

Figure 28. Wheel life testing was performed in the JPL Mars Yard using a three-wheel test rig with rocker and bogie suspension arms and a front, middle, and rear wheel. Image Credit: NASA/JPL-Caltech

wheel surface and the wheel actuator cable. The base of flap LM-4 is folded at grouser 13, therefore, flap LM-4 cannot grow any longer.

5. How Wheel Damage Assessment Has Influenced Driving Guidelines

After completing the first FMWI on sol 490 and convening the Tiger team, the MSL Operations team put numerous constraints in place with the goal of minimizing wheel damage while the Tiger team conducted its investigation into the mechanics of wheel wear. These constraints and practices changed and evolved quickly as the team's understanding of wheel wear improved. Drive distance was restricted to distances over which terrain could be evaluated by RPs during the drive planning process. This effectively restricted the use of Curiosity's autonomous navigation (AutoNav) driving modes which conduct terrain safety assessments in real time at distances beyond what can be evaluated for safety by RPs. Drives during this period of time were typically less than 30 m. Beyond that distance, it was difficult to identify high-risk rocks to wheel damage in navigation camera images. The team also captured SPMWI as often as possible, after or between drives along the strategic route.

Figure 28 illustrates a three-wheel test rig used in the Mars Yard to perform wheel life testing [5]. As Mars Yard testing confirmed the role of small, pointed, embedded rocks on accruing wheel damage, the strategic route planning team altered the route planned for the rover with the goal of transitioning to more wheel friendly terrain without significantly increasing total drive distance towards the next goal. Use of AutoNav and multi-sol driving was formally restricted on sol 516.

The Operations team also implemented a policy to maximize backwards driving, which was proven to reduce wheel damage to the middle and front wheels at the expense of increasing damage to the less worn rear wheels. Driving backwards increases the duration and complexity of a drive due to the added time for additional turning and terrain imaging. SPMWI continued to be performed at 30 m intervals, while FMWI, initially requested at approximately 100 m intervals, was increased to 200 m on sol 537.

Additional testing informed the team that the extra odometry accumulated on the wheels while turning (which requires steering the front and rear wheels in place) negated the advantages of driving backwards. The emphasis on prioritizing backward driving was removed under conditions where terrain is rated as benign or when there are no areas that allow for turning at low cost to the wheels. Current Wheel Wear Driving Guidelines:

1. Minimize Turning
   - Drive forward in benign terrain.
   - In challenging terrain, drive backwards if there are areas of benign terrain which allow for the turning at low cost to the wheels. Otherwise drive forward.
2. AutoNav is permitted for single sol use in any traversable terrain
   - No distance restriction on AutoNav as long as the rover is constrained to stay on strategically approved terrain. RPs and Surface Properties Scientist (SPS) may extrapolate to unseen terrain based on ground images and homogenous terrain from orbital images.
3. Minimize wheel contact with embedded rocks that can results in single points of contact.
4. When driving on loose material, minimize wheel contact with rocks taller than 8 cm that could result in a single point of contact. Smaller rocks are expected to be depressed into the terrain and are less of a threat to the wheels.

To facilitate strategic route planning with the reduction of wheel damage in mind, extensive efforts were made to map the different terrain types making up the preferred MSL route in conjunction with geologists on the MSL science team. Mars Yard wheel testing along with damage rate data provided by FMWI assessments informed the classification of different types with respect to their likelihood to cause wheel damage. This allowed the Operations team to select paths that biased the rover away from travelling over regions identified as ”Irregular Sharp Outcrop”, the most threatening to wheel health [6]. Terrain classifications for wheel wear were updated and revised frequently over the next few years of the MSL mission.

One goal of wheel wear terrain classification was the creation of a predictive damage model based on terrain type. Using wheel wear crack measurements accumulated with every FMWI since sol 490 and damage curves from different terrain types tested in the Mars Yard, the Wheel Wear team established a numerical ranking scale for different terrains. The model went into use on sol 1127. The goal of the scale was to capture the approximate rate of damage growth seen driving over different terrains and use the rates to estimate the impact of future drive routes on wheel wear. The range of values (1-10) capture uncertainty or error in the damage scale due to potential differences in specific interactions between rock, substrate, and wheel. The original terrain rankings were modified on sol 1798 to account for an additional 6 km of wheel wear data. The majority of driving during this period was spent on variations of Murray Formation terrain. Both sets of ratings are shown in Table 6.

Since reaching approximately 11,000 m on the surface of Mars, wheel damage rates have remained consistently lower than terrain classification-based predictions, even as the rover has traversed multiple distinct geologic regions. This is attributed to RP drive guidelines effectively preventing MSL from driving over sharp embedded rocks along with an overall reduction in terrain risk. A large percentage of early mission driving was done on caprock on the plains. The transition onto the softer bedrock of Mount Sharp (Murray Formation) marked a key inflection point in the damage curves of the front and middle wheels. Most wheel wear accumulated since leaving the Pahrump Hills region at 11,000 km is associated wheel interactions with small pebbles and occasional unavoidable rocks that are largely terrain type independent. Further attempts to reclassify terrain types with respect to wheel wear were made in 2019, but did not result in a more accurate model when compared to historical damage rates. Use of the wheel wear terrain classification ratings as a tool for estimating future damage rates was discontinued after the sol 2592 FMWI.

Table 6. Terrain Classification Damage Ratings

Terrain Class	**Description**	**Rating Released Sol 1127**	**Rating Updated Sol 1798**
Ripples	Sandy	1	1
Smooth	Sandy, small rocks will press into substrate	1-3	1-3
Smooth with Rocks	Sandy, avoidable large rocks	3-4	3-4
Murray Formation	Hard and smooth, size of loose rocks on surface determines range of wheel damage	6-10	2-6
Caprock Smooth	Hard substrate with sand patches	6-7	4-5
Caprock	Hard substrate with embedded rock	7-9	4-7
Caprock Rough	Hard substrate with a high density of embedded rock	7-10	5-8
Rock Field	Ranges from loose rock scattered in sand to large embedded rocks in substrate	4-9	4-9

Following the sol 1512 FMWI (15,080 m driven), the required cadence of wheel imaging was reduced significantly in response to a drop-off in wheel damage rate. Regular SPMWI was discontinued and became an activity only executed if requested by the Wheel Wear team. The FMWI cadence was updated to occur every 500 m.

Performing FMWI is a resource expensive activity to perform on Mars. The activity itself can take between 2 and 2.5 hours to execute and requires the repeated unstowing and stowing of the robotic arm between short drives to capture images of the wheels in all five positions. Given the consistent rate of damage seen over the course of several years, the FMWI cadence was reduced again to 1000 m on sol 2781, which has remained the cadence as of sol 3195.

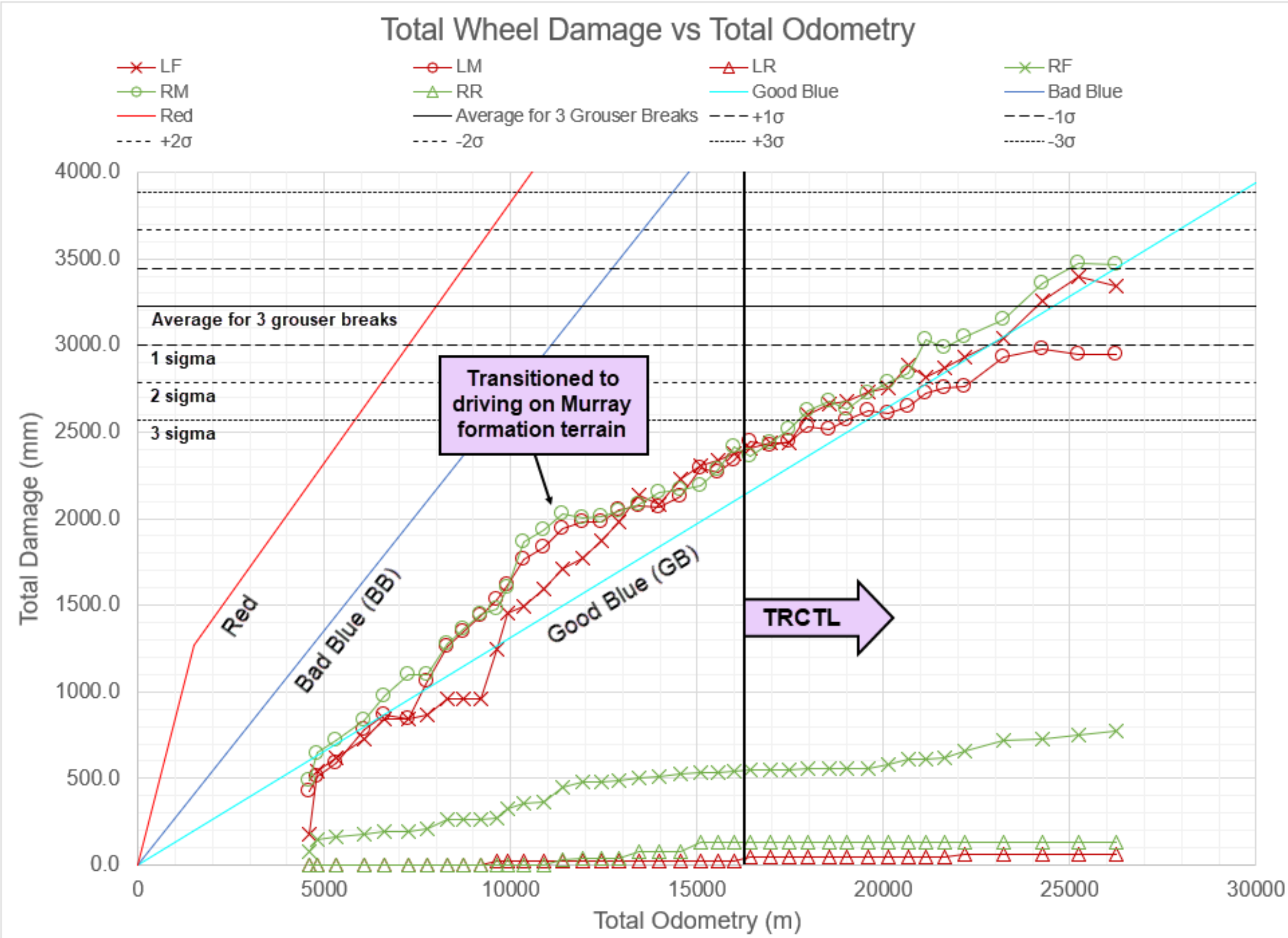

Figure 29. Wheel Damage vs Distance Driven as of the sol 3195 FMWI.

While damage rates have remained approximately linear for several years and many kilometers of driving, several major milestones in wheel life have been observed. The sol 1641 FMWI image set revealed the first two broken grousers on the LM wheel just a few sols before the first TRCTL checkout test on Mars on sol 1646. Tiger team testing established three broken grousers on a single wheel as a significant wheel life milestone, equating to a wheel reaching 60% of its life. The Wheel Wear team's primary goal is to extend the life of Curiosity's damaged wheels so the mobility system can continue to support MSL's extended mission science objectives.

The historical damage rate of the flight vehicle's wheels is typically compared to the rate of damage seen by the "Good Blue" test wheel, a wheel driven to failure during wheel life testing on artificial terrain with a moderate damage risk rating. The color rated terrains were created by terrain scientists on the Tiger Team to best represent the range of terrain severity Curiosity had driven on to that point, with Good Blue and Bad Blue differentiating the least and most harsh variations of nominal driving terrain. Good Blue would rate a 4-5 on the terrain classification scale developed later, while Bad Blue would rate 7-8. The Good Blue test wheel serves as a convenient reference to the flight wheels because its damage rate expressed as growth of total crack length over distance driven is comparable to the linear rates observed in flight for the last 15 km of driving.

Two metrics derived from wheel life testing are used to compare the state of the flight wheels to test articles:

1. Total damage accumulated on a wheel
2. Distance driven since the first broken grouser.

Wheel life testing identified 3200 mm as the average amount of damage seen on a single wheel when its 3rd grouser broke. As of sol 3195, the latest FMWI as of this publication, wheels LF, LM, and RM are all within +/- 2 standard deviations of this value, but only LM has experienced 3 broken grousers. The second metric estimates that the 3rd broken grouser could be expected on a wheel 3.6 km after the first break is seen. LM, by comparison, drove 9.2 km before the 3rd break was seen on sol 3079. These trends speak to the efficacy of TRCTL and RP driving guidelines reducing the frequency and likelihood of the high energy terrain interactions required to break wheel grousers. Figure 29 shows the damage accumulation on all 6 wheels over the course of the mission.

Wheel life testing indicates that performance degradation of a single wheel and its impact on the mobility system performance as a whole is not seen until all 19 grousers are broken on a single wheel. Of particular concern is the loss of structural integrity of the wheel at end-of-life, which poses a threat to the rest of the mobility system hardware, including the drive and steer actuators. Testing conducted in 2018 determined that if a wheel reaches the heavily damaged state of 19 broken grousers, the broken sections of the wheel can be removed in-situ through a process called Wheel Shedding, further extending the life of the wheel beyond 19 broken grousers. It is not expected that this will be required on MSL. The milestone for deciding whether to pursue Wheel Shedding in flight is when 14 broken grousers are seen on a single wheel [9].

The rate of broken grousers of the Good Blue test wheel is used as a worst-case estimate for when LM could reach the 14 broken grousers milestone. Flight data has already demonstrated that LM's broken grousers are well below the pace of Good Blue. Also factored into this prediction is the estimated reduction in drive distance per year as the MSL rover continues to age. MSL's Multi-Mission Radioisotope Thermoelectric Generator (MMRTG) power source output decays over time, reducing the amount of energy available each day for science and engineering activities on Mars. One impact of the reduction in available power is an inability to maintain MSL's historical 3 km/yr drive rate. As wheel damage and broken grouser estimates are a function of distance driven, the reduction in drive rate will lengthen the estimated remaining life of the wheels.

6. SUMMARY

After notable damage to Curiosity's wheels was observed early in the mission, FMWI was developed as a routine activity to assess and quantify wheel wear. It is the primary means of understanding the rate of wheel damage, an increase in which could restrict drive distance resulting in reduced science return. FMWI is a manually intensive process, so there is a continuing need to improve its efficiency as the mission's resources shrink. The most recent FMWI on sol 3195 provided the mission with an update on the current state of Curiosity's wheels after 26.3 km of driving. Curiosity currently has several large skin sections missing and a total of 4 broken grousers, three on the LM wheel and one on the RM wheel. That's significantly less than the 14 grouser breaks predicted on a single wheel after 24 km of driving [10].

Because Curiosity has recently been trending below wheel damage predictions, the FMWI cadence has been relaxed relative to requirements earlier in the mission. In addition to the development of FMWI, several operational strategies were initially pursued to reduce the rate of wheel damage. The most effective of these has proved to be hazard avoidance. The RPs avoid hazards by identifying sharp obstacles and intentionally navigating around them. The reduced damage rate is also attributed to the implementation of the TRCTL driving algorithm. Other mitigation strategies such as terrain classification and SPMWI were developed but were eventually retired due to lack of added value.

Although Curiosity's wheels continue to accumulate damage as the rover continues to drive across mixed Martian terrain, an individual wheel can absorb significant damage before it causes any impact to mobility performance. Testing in the JPL Mars Yard on the Scarecrow testbed rover [11] indicates that Curiosity could continue to drive indefinitely on the portion of a wheel that remains when all the grousers on a wheel breaks, if the unconstrained portion of the wheel can be safely shed [9].

The wheels for the Mars 2020 (M2020) Perseverance rover were redesigned with knowledge from MSL to prevent it from experiencing wheel damage as severe as its older sibling. Figure 30 contains a side-by-side view of a Curiosity wheel and a Perseverance wheel. Most notably, the Perseverance wheel has skin that is more than twice as thick and has nearly twice as many grousers. Over the first eight months of Mars 2020 surface operations (as of sol 223), Perseverance has driven 2,663.7 meters. As expected, no wheel damage has been observed. Although TRCTL has been implemented as a patch for Perseverance, it would require additional validation testing if a decision was made to use it on Perseverance.

Figure 30. Side-by-side view of a Curiosity and Perseverance wheel. Image Credit: NASA/JPL-Caltech.

ACKNOWLEDGMENTS

The research described in this paper was performed at the Jet Propulsion Laboratory, California Institute of Technology, under contract with the National Aeronautics and Space Administration. The authors would like to thank the Mars Science Laboratory Program for supporting this research, Howard Eisen for providing MPF wheel documentation, Patrick Degrosse for providing MSL and M2020 wheel documentation, and Matt Heverly for discussions related to wheel wear.

REFERENCES

[1] A. Rankin, M. Maimone, J. Biesiadecki, N. Patel, D. Levine, and O. Toupet, "Driving Curiosity: Mars rover mobility trends duing the first seven years," in *IEEE Aerospace Conference*, Big Sky, Montana, USA, Mar. 2020.

[2] D. Bickler, "Roving over Mars," *ASME Mechanical Engineering Magazine*, vol. 120, no. 4, pp. 73–77, Apr. 1998.

[3] E. Tunstel, M. Maimone, A. Trebi-Ollennu, J. Yen, R. Petras, and R. Willson, "Mars Exploration Rover mobility and robotic arm operational performance," in *IEEE International Conference on Systems, Man and Cybernetics*, Waikoloa, Hawaii, USA, Oct. 2005.

[4] S. Haggart and J. Waydo, "The mobility system wheel design for NASA's Mars Science Laboratory mission," in *11th European Conference of the International Society for Terrain-Vehicle Systems*, Torino, Italy, Nov. 2008.

[5] R. Rainen, "Mars Science Laboratory wheel damage mechanical tiger ream final report," Nov. 2015, MSL Internal Document.

[6] R. Arvidson, P. DeGrosse, J. Grotzinger, M. Heverly, J. Shechet, S. Moreland, M. Newby, N. Stein, A. Steffy,

F. Zhou, A. Zastrow, A. Vasavada, A. Fraeman, and E. Stilly, "Relating geologic units and mobility system kinematics contributing to Curiosity wheel damage at Gale Crater, Mars," *Journal of Terramechanics*, vol. 73, pp. 73–93, Oct. 2017.

[7] E. Lakdawalla, "Curiosity wheel damage: The problem and solutions," https://www.planetary.org/articles/08190630-curiosity-wheel-damage, Aug. 2014, accessed: 2021-11-07.

[8] O. Toupet, J. Biesiadecki, A. Rankin, A. Steffy, G. Meirion-Griffith, D. Levine, M. Schadegg, and M. Maimone, "Terrain-adaptive wheel speed control on the Curiosity Mars rover: Algorithm and flight results," *Journal of Field Robotics*, vol. 37, no. 5, pp. 699–728, Aug. 2020.

[9] E. Graser, S. McGill, A. Rankin, and A. Bielawiec, "Rimmed wheel performance on the Mars Science Laboratory Scarecrow rover," in *IEEE Aerospace Conference*, Big Sky, Montana, Mar. 2020.

[10] A. Steffy, "Wheel wear strategic plan," Oct. 2016, MSL Internal Document.

[11] M. Heverly, J. Matthews, J. Lin, D. Fuller, M. Maimone, J. Biesiadecki, and J. Leichty, "Traverse performance characterization for the Mars Science Laboratory rover," *Journal of Field Robotics*, vol. 30, no. 6, pp. 835–846, Sep. 2013.

BIOGRAPHY

Arturo Rankin *received his Ph.D. in Mechanical Engineering at the University of Florida in 1997. He is currently a Robotic Systems Engineer in the Robot Operations group at the Jet Propulsion Laboratory, and the M2020 Robot Operations deputy lead. Prior to that, he was the MSL Mobility/Mechanisms team lead and the MSL Flight Software team lead.*

Nikunj Patel *is a Tactical Downlink Lead for MSL, which follows the responsibilities of a flight director on the mission. In addition to that, he is also the Mobility Subject Matter Expert and the Wheel Wear team lead for Curiosity Rover. He received his Masters in Aerospace Engineering from University of Central Florida (UCF) where he led multiple cubesatellite development machines through AIAA and UCF. In addition to that, Nikunj designed the first Ground Support Biobarrier (GSB) that would be utilized by NASA's Planetary Protection (PP) team to meet stringent bioburden requirements for future life detection missions to other terrestrial bodies.*

Evan Graser *is a Systems Engineer in the Engineering Operations for Surface Missions group at JPL. He is currently the MSL Mobility/Mechanisms subsystem team lead and the deputy lead of the M2020 Perseverance Mobility downlink team. He is a member and the lead trainer of the MSL Engineering Operations Systems team. Evan received is MS in Aerospace Engineering from the University of Colorado, Boulder.*

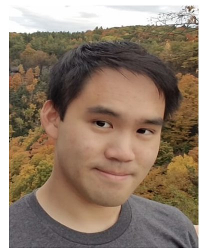

Jiun-Kai Freddy Wang *is a Mechatronics Engineer in the Mechanisms and Mobility group at JPL. He built and tested MSL heritage actuators and seal dispensing mechanisms for the Mars 2020 mission before joining MSL as a member of the Mobility/Mechanisms subsystem team. He received his Bachelor of Science in Mechanical Engineering from Rensselaer Polytechnic Institute.*

Kimberly Rink *is a Systems Engineer in the Engineering Operations for Surface Missions group at JPL. She currently leads the Fault Protection subsystem team, operates and maintains the vehicle and mission systems testbeds, and is a member of the Mobility/Mechanisms subsystem team for MSL. Kim received her MS in Aeronautics and Astronautics from Purdue University.*